DECONVOLUTING AN AMERICIUM-BERYLLIUM NEUTRON SPECTRUM FROM A PROTON RECOIL DETECTOR

A Thesis

by

YESENIA AMANDA GONZALEZ

Submitted to the Office of Graduate and Professional Studies of
Texas A&M University
in partial fulfillment of the requirements for the degree of

MASTER OF SCIENCE

Chair of Committee, John Ford
Co-Chair of Committee, John W. Poston, Sr.
Committee Member, Nancy Turner
Head of Department, Yassin A. Hassan

December 2016

Major Subject: Nuclear Engineering

ABSTRACT

A proton recoil detector was acquired from LND, Inc. to be used in neutron counting experiments with an ^{241}AmBe source. Neutrons elastically scatter off of and ionize hydrogen atoms creating protons that can be detected. A single neutron can undergo multiple scattering events and this can result in several pulses being registered by the detector. This method of detection creates a detector response that changes with varying neutron fields, and unless both the incident neutron field and detector response to the neutron field are known, then it is not possible to visually determine what the detector is measuring.

In order to solve this problem, we attempted to unfold the measured spectrum using MAXED. MAXED requires the measured spectrum, as well as a file containing response functions. Since there was no access to monoenergetic neutron sources to experimentally determine these response functions, the response functions were calculated using MCNPX. In addition, the detector response to several different ^{241}AmBe neutron spectra were calculated and compared to the experimental data.

Using MCNPX, the detector response was able to be modeled. Unfolding the experimental data was not successful, but the MCNPX results are consistent with the detector measuring an ^{241}AmBe spectrum. The actual ^{241}AmBe neutron spectrum can vary from source to source, so the spectrum used in MCNPX is not necessarily the spectrum emitted by the ^{241}AmBe source. For future experiments and simulations using this specific source, the results of the MCNPX simulation can serve as a starting point for the neutron energy distribution. There will still be uncertainty associated with the source in simulations; however, with the number of different ^{241}AmBe source spectra available, using a spectrum that produces results that match experiments can

help reduce the error in future simulations.

NOMENCLATURE

MCNP	Monte Carlo N-Particle
eV	Electronvolt
UMG	Unfolding with MAXED and GRAVEL
MeV	Megaelectronvolt
Ci	Curie
HDPE	High Density Polyethylene
CSDA	Constant Slowing Down Approximation
SRIM	Stopping and Range of Ions in Matter
LANL	Los Alamos National Laboratory

TABLE OF CONTENTS

Page

LIST OF FIGURES

FIGURE Page

1. INTRODUCTION

Neutron counting experiments were performed at the Nuclear Science Center using a ^{241}AmBe neutron source and a proton recoil detector acquired from LND, Inc. Due to the way the detector functions, the spectrum changes with varying neutron fields and because of this, it is not possible to tell whether the spectrum produced by the detector is a result of it actually measuring the ^{241}AmBe neutron source, or if the shape is distorted by electronic noise. It is believed that the detector and electronics are functioning properly, however, in order to verify this, MCNP was used to simulate the detector response.

1.1 Literature Review

There are many methods that can be used for neutron detection, however, these methods vary depending on the energy of the neutron. Neutrons contain no charge and are unable to be directly detected. Because of this,neutrons must interact with another particle which is then able to be detected. Scattering and absorption interactions can be taken advantage of for neutron detection purposes. [1] As neutron cross sections are energy dependent, the method of detection can vary with the energy of the incident neutron.

For neutrons with energy less than 0.5 eV, or thermal neutrons, they are usually detected via nuclear reactions. [2] In a BF_3 detector, neutrons are detected via a^{10}B(n,α)^{7}Li reaction which produces a characteristic spectrum as shown in Figure 1.1.

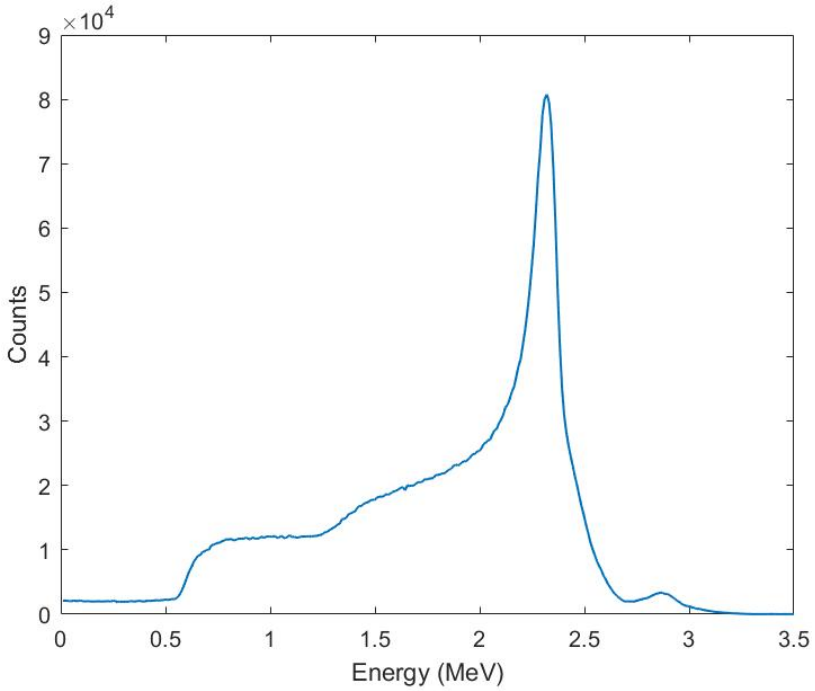

Figure 1.1: BF_3 detector response to neutrons.

Similar to the BF_3 detector, ^{3}He detectors rely on a neutron absorption reaction, ^{3}He(n,p)^{3}H. [2] While these are common methods for thermal neutron detection, there is no way to obtain any information regarding the energy of the incident neutron.

Another method for fast neutron detection is to detect the recoil nuclei from elastic scatterings. [2] This method is better for faster neutrons than thermal neutrons as the energy of the recoil nuclei from thermal neutrons is quite small. [2]

1.1.1 Proportional Counters and Proton Recoil Detectors

Proportional counters are gas-filled detectors that rely on gas multiplication to amplify the signal. As the applied voltage to the detector is increased, the probability of ions creating secondary ions increases. Those secondary ions might then be able

to create more ions and so on in a process known as a Townsend avalanche. The number of secondary ions created is proportional to the number of original ions created within the detector volume over a limited voltage region. [2]

Proton recoil detectors are proportional counters that rely on the elastic scattering of neutrons that create a recoil nucleus that is detectable. As they rely on scattering events rather than absorption events, the detectors are able to detect neutrons above the thermal range, 0.025 eV. Energy transferred from the neutron to the recoil nucleus can be related through Equation 1.1 where A is the atomic mass number, E_n is the energy of the incident neutron, and θ is the scattering angle. [2]

$$E_R = \frac{4A}{(1+A)^2}\cos^2(\theta)E_n \tag{1.1}$$

The energy transferred to the recoil nucleus is dependent on the scattering angle of the recoil nucleus, and the maximum energy transfer occurs when θ is equal to zero degrees, or in a head-on collision. The maximum energy transfer, $E_{R_{Max}}$, in a head-on elastic collision is shown by Equation 1.2.

$$E_{R_{\mathrm{Max}}} = \frac{4A}{(1+A)^2}E_n \tag{1.2}$$

For a proton recoil detector filled with hydrogen gas, 100% of the energy of the incident neutron can be transferred to the recoil proton in a head-on collision. The energy distribution of the recoil nucleus can be determined using Equation 1.3.

$$P(E_R) = \frac{(1+A)^2}{A}\frac{\sigma(\theta)}{\sigma_s}\frac{\pi}{E_n} \tag{1.3}$$

Here $\sigma(\theta)$ is the differential scattering cross section, and σ_s is the total scattering cross section. [2] In a detector filled with hydrogen, $\sigma(\theta) = \frac{\sigma_s(\theta)}{4\pi}$ since neutrons

are scattered isotropically in the center of mass frame. [3] With this, Equation 1.3 can be simplified and written as Equation 1.4 which shows that for monoenergetic neutrons, the detector response will be rectangular. While this is what the spectrum would look like ideally, there are factors, such as multiple particle scatterings, that can distort this shape. [2]

$$P(E_R) = \frac{1}{E_n} \tag{1.4}$$

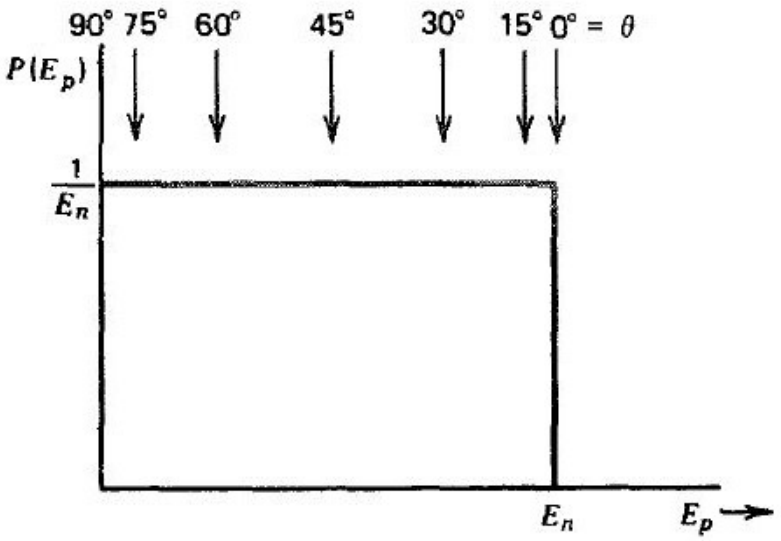

Figure 1.2: Expected response from a monoenergetic neutron source. [2]

1.1.2 UNFOLDING

The convolution of two functions, $f(t)$ and $g(t)$, can be written as shown in Equation 1.5. [4]

$$h(t) = (f * g)(t) \tag{1.5}$$

For this application where $f(t)$ and $g(t)$ are expressed as the response function of the detector and the source spectrum and $h(t)$ is the measured spectrum. The process of deconvoluting involves solving the integral shown in Equation 1.6 where M(E) is the measured source spectrum (pulse height distribution), S(E') is the source spectrum, and R(E,E') is the response function of the detector. [5]

$$M(E) = \int_0^\infty R(E, E')S(E')dE' \tag{1.6}$$

The detector response function is the pulse height distribution that is produced in response to a monoenergetic source and can be determined experimentally using a monoenergetic source of the radiation of interest, but when such a source is not available, the response function can be modeled and calculated through the use of programs such as MCNP. [2] Response functions are detector specific and should be calculated or measured for each detector.

While solving for the source spectrum is simple for monoenergetic neutron sources, sources with an energy distribution can require the use of unfolding programs to solve for the source spectrum.

1.1.2.1 UNFOLDING CODES

UMG created by Physikalisch-Technische Bundesanstalt in Germany. There are two versions of MAXED and GRAVEL, a "few-channel" and a "multi-channel" version. This software runs on Windows® software up to Windows XP®. To run MXD or GRV, three input files are needed: a file with the measured data, a file with the detector response functions, and a file with a default flat-line spectrum. [6]

MXD_MC33 processes data until some values, λ_k, are found that solve the following equations. N_k is the measured counts, σ_k is the estimate of the measurement error, f_{DEF} is the default spectrum, R_{ki} is the detector response, and Ω is a parameter

that fixes the X^2 of the solution. [6]

$$N_k + \epsilon_k = \sum_i R_{ki} f_i \tag{1.7}$$

$$\sum_k \frac{\epsilon_k^2}{\sigma_k^2} = \Omega \tag{1.8}$$

$$f_i = f_i^{DEF} \exp\left(- \sum_k \lambda_k R_{ki} \right) \tag{1.9}$$

$$\epsilon_k = \frac{\lambda_k \sigma_k^2}{2} \left(\frac{4\Omega}{\sum_j (\lambda_j \sigma_j)^2} \right)^{\frac{1}{2}} \tag{1.10}$$

In addition to UMG, there are other unfolding programs available that use a least squares method to solve the equation where Φ is the measured spectrum, R is the detector response function, and N is the incident neutron spectrum. [7]

$$\Phi = R^{-1} N \tag{1.11}$$

1.1.3 MCNP

MCNP is a Monte Carlo radiation transport code created at Los Alamos National Laboratory that is capable of simulating the transport of many types of particles. MCNP was first released in 1977, and the latest version, MCNP6.1, was released in 2013. [8] MCNP-PoliMi was released in 2004 and expanded on the neutron interactions within organic scintillators and included options not available before, such as accounting for recoil nuclei. Some of the features of MCNP-PoliMi were added to the latest version of MCNPX, version 2.7.0. [9]

2. EXPERIMENTAL SETUP AND MCNP

2.1 Description of Experimental Setup

The experiments were performed using a spherical proton recoil neutron detector Model 27044 manufactured by LND, Inc, as seen in Figure 2.1. The filling gas for this detector is hydrogen at a pressure of 2280 torr. The chamber has a diameter of 5.08 cm. The proton recoil detector was connected to an Ortec 142PC preamplifer, which was then connected to an Ortec 570 pulse shaping amplifer with a shaping time set at 3 μs and a gain of 200 mV. The output was split between two different acquisition systems: one with an Ortec 550A single channel analyzer and an Ortec dual counter/timer, and the other with a Canberra Multiport II MCA controlled by Genie 2000^{TM} software. The voltage for the proton recoil detector was set at +2.75 kV using a Canberra 3106D power supply. (See Figure 2.2)

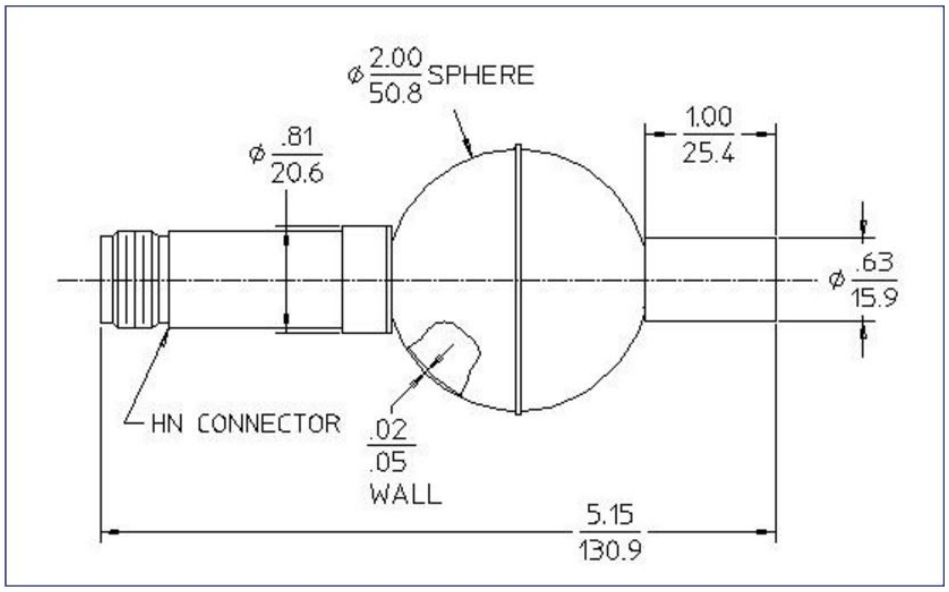

Figure 2.1: Schematic of the proton recoil detector purchased from LND, Inc.

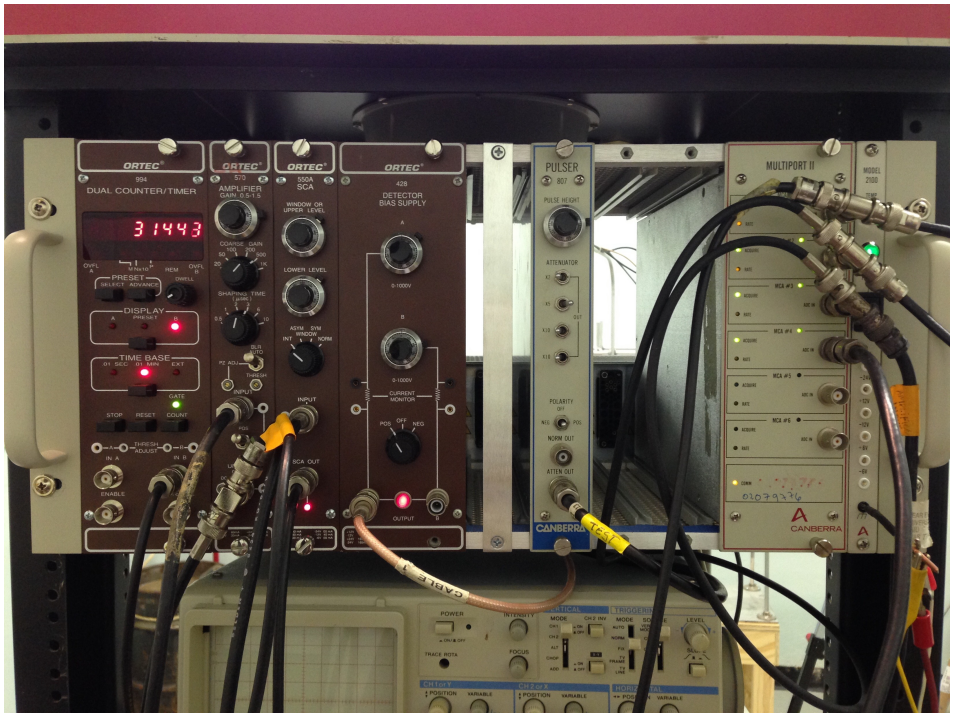

Figure 2.2: NIMBIN module used in the experiment.

An ^{241}AmBe source (MRC-AmBe-1280) was used during the experiment. It is a continuous source that emits neutrons up to 11 MeV with an average energy 4.2 MeV. [10] In addition to neutrons, the ^{241}AmBe source emits a 4.4-MeV gamma ray that is capable of interacting with the stainless steel cathode or the fill gas, and able to produce electrons that contribute to noise. [1] The neutron spectrum of a typical source is shown in Figure 2.3.

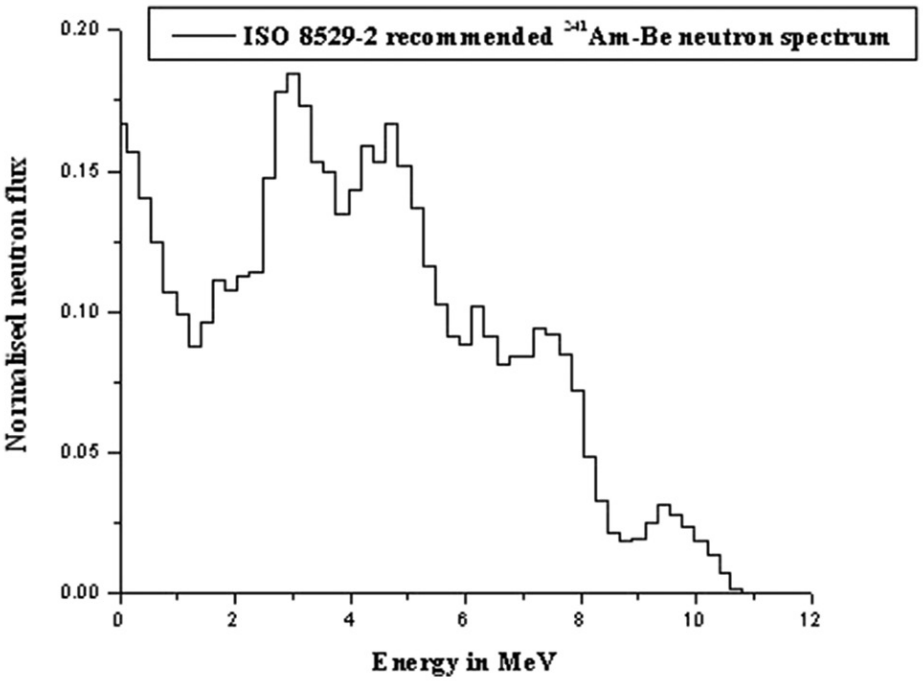

Figure 2.3: Neutron emission spectrum of an AmBe source. [11]

The ^{241}AmBe source was located within a cylindrical stainless steel casing approximately 5.08 cm tall and 2 cm in diameter with an initial activity of 2.52 Ci on November 9, 1972. [12] The actual size and distribution of the ^{241}AmBe mixture within the stainless steel casing is unknown.

For the measurements, the ^{241}AmBe source was placed in the center of a HDPE cylinder with the base of the source 7.62 cm from the base of the cylinder. The HDPE cylinder was surrounded by a 1.27 cm thick layer of borated HDPE. The HDPE cylinders were located on a 0.64 cm thick layer of boral that was placed on top of a wooden table 64 cm tall. The lowermost point of the proton recoil detector was placed approximately 46 cm from the top of the boral plate as seen in Figure 2.4.

The experiments were performed at the Nuclear Science Center and were subject to a changing environment since the reactor was powered on and off at least once a day. Several measurements were taken, ranging between one hour and 15 hours.

Figure 2.4: Experimental setup with the source in the HDPE shield (left) and in the minimalist configuration (right).

2.2 Description of MCNP Deck and Assumptions

An input deck was created using MCNPX version 2.7.0. The detector was modeled following the specification sheet provided by LND, Inc. [13] Instead of modeling the 5.08 cm tall cylindrical ^{241}AmBe source where the source distribution within the steel casing is uncertain, the source was instead modeled as a flat circular plane with a diameter of 2.6 cm. To simplify the problem, only the detector and the source were modeled as can be seen in Figure 2.5.

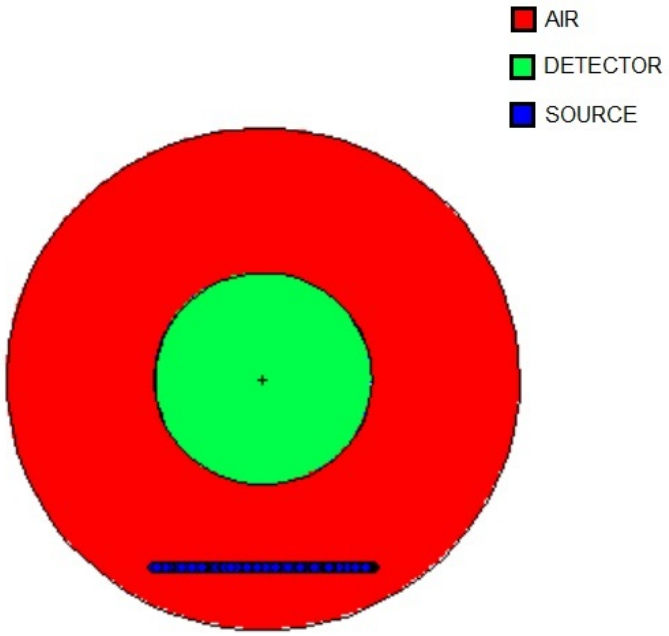

Figure 2.5: Geometry of modeled experiment.

The MCNPX deck was run with mode N (neutrons), H (protons), P (photons), and # (heavy-ions). The physics option for neutrons and protons was needed in the input deck since MCNP does not account for recoil nuclei based on the default settings.

The PHYS:N and PHYS:H were required in the input deck to allow for the simulation of recoil nuclei. A combination of F6, energy deposition, and F8, pulse height, tallies were used. The F6 tallies were used to calculate the deposited energy from the protons in the fill gas and in the stainless steel detector walls. The F8 tally was used as a way to model to the pulse height distribution of the detector, however,

it required the PHL option to combine the results from the two F6 tallies. The F8 tally was also modified using an FT CAP tally which forces the simulation to run in an analog mode. Running in analog mode does not allow for variance reduction and is required for the F8 tally. [14]

MCNPX was run using an ISO ^{241}AmBe spectrum to simulate the experimental result. The simulation was run using 2.0x10^{9} particles. To calculate the response functions, 120 different monoenergetic neutrons between 0.15 MeV to 11 MeV were run individually. Following the monoenergetic neutron runs, the results were processed through Matlab® to smooth the response using the moving average filter, and then re-sized into a 7 x 147 matrix. The re-sizing of the matrix was necessary to format it accordingly for the response function file as determined by MAXED.

2.3 MAXED

UMG was obtained online from RSICC and contained both MAXED and GRAVEL software. MAXED works on Windows® platforms up to XP. Since XP software was not readily available, it was necessary to run the XP Virtual Machine on Windows® 7. Once MXD_MC33 was installed it was run using a control file that specified the location of the needed input files and the parameters needed to run the problem. The three input files needed by MAXED are: a file with the measured response, a file with the response functions, and a file with the default spectrum. The measured response was taken from the experimental results, the single response function file was created with the results of all 120 response functions calculated using MCNPX, and the default spectrum was a flat-line, as provided by MAXED.

In addition to the input files, the boundaries of the response functions and measured data need to be specified as well as, a chi-square per degree of freedom, a number of iterations to use, a user-specified energy bin structure for the solution,

and whether to scale the default spectrum, and what to scale it by, if needed.

The measured data has three reserved lines that contain a description of the data in the first line, the units and form (fluence rate per bin) of the measured data in the second line, and the number of channels and energy boundaries in the third line. Following this, the energy, pulse height, and uncertainty of the pulse height were added in three columns. The response function file contains two reserved lines, the first being the width of the energy bins in MeV, and the second line containing the energy of the incident particle, the number of channels, and the energy boundaries for the data. A 7 x 147 detector response matrix was added specifying the incident neutron energy. Each new incident particle energy was specified prior to adding the data. The default spectrum follows the exact format as the measured data file.

Running MAXED results in the creation of four files, .txt file with unfolding information, a .plo solution spectrum, .flu differential solution spectrum, and a .par that is able to be used as an input file for a separate program included with UMG.

3. RESULTS AND DISCUSSION

3.1 Experimental

In order to determine the maximum energy of a proton that can fully deposit its energy within the detector, the density of hydrogen gas inside the detector was calculated using the ideal gas equation shown in Equation 3.1.

$$PV = nRT \tag{3.1}$$

Here P is the pressure in the detector, V is the volume of the detector, n is the moles of hydrogen gas, R is the ideal gas constant, and T is the temperature. Substituting Equation 3.2 into the ideal gas equation allowed the density, ρ, to be calculated directly using the detector parameters where m is the mass of hydrogen within the detector, and M is the molar mass of hydrogen.

$$n = \frac{m}{M} \tag{3.2}$$

Inserting the following values of M=2 g/mol, T=300 K, R=62363 cm^3 torr/K/mol, and P=2280 torr into Equation 3.3 led to a calculated density of 2.44x10^{-4} g/cm^3.

$$\rho = \frac{PM}{RT} \tag{3.3}$$

Using the diameter of the detector and the calculated density of the hydrogen gas, the CSDA range can be calculated using Equation 3.4 where ρ is the density of

the hydrogen gas in the detector, and R is the range of the proton in the hydrogen gas. [15]

$$R\rho = CSDA \tag{3.4}$$

Using the calculated density of the hydrogen gas and the diameter of the detector as the range of the proton, the CSDA range was calculated to be 1.24x10^{-3} g/cm^2. The CSDA values from NIST were used to determine that, at most, a 1.24 MeV proton can fully deposit its energy within the detector volume. By rearranging Equation 3.4 into Equation 3.5, the range for the maximum and average neutron energies can be calculated.

$$R = \frac{CSDA}{\rho} \tag{3.5}$$

The range of an 11 MeV proton was calculated to be 260.98 cm, and the range of a 4.2 MeV proton was found to be 44.96 cm.

$$Range_{11\text{ MeV}}(cm) = \frac{6.36x10^{-2}g/cm^2}{2.44x10^{-4}g/cm^2} = 260.98cm$$

$$Range_{4.2\text{ MeV}}(cm) = \frac{1.097x10^{-2}g/cm^2}{2.44x10^{-4}g/cm^2} = 44.96cm$$

The ranges were confirmed by using SRIM, a software that is able to calculate the range of ions in various media. The output provided a list of the proton range for

energies ranging from 0.01 MeV to 10 MeV in the previously calculated density. This was able to be plotted as a function of energy as seen in Figure 3.1.

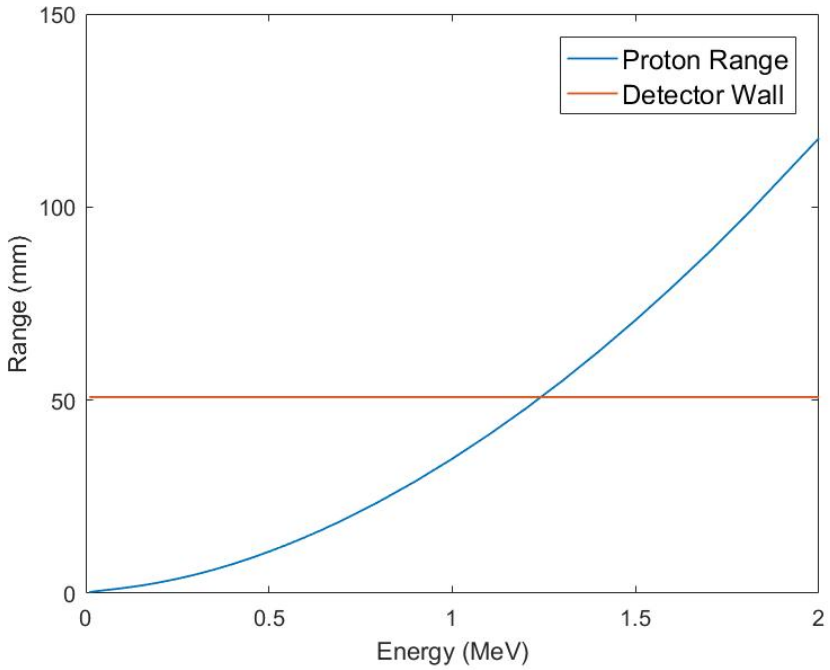

Figure 3.1: Range of protons at various energies in hydrogen gas.

After setting up the experiment, the ^{241}AmBe source was removed from the room and a background measurement was started and counted for 15 hours with the gain set at 100. The background spectrum can be seen in Figure 3.2.

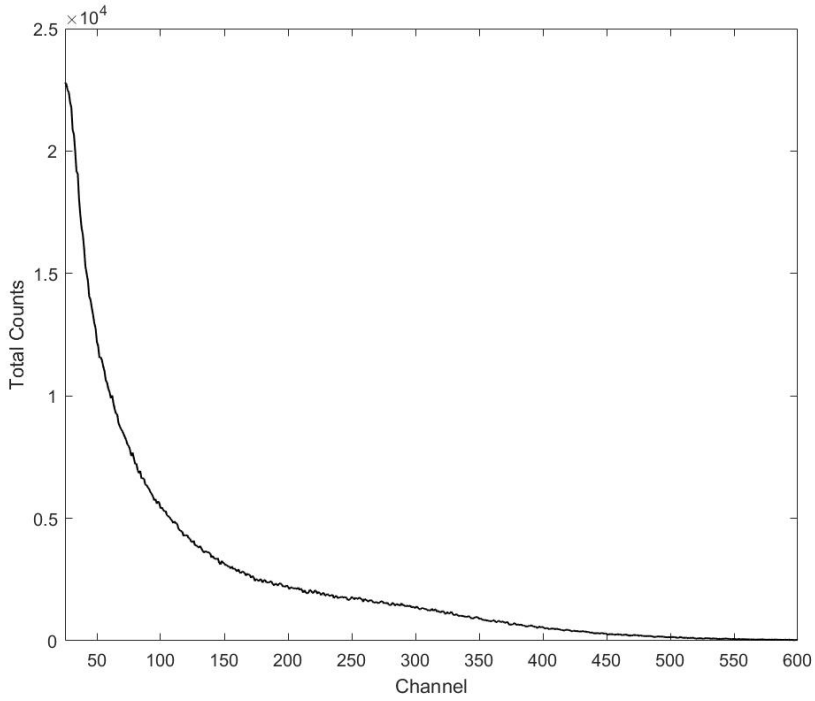

Figure 3.2: Proton recoil detector response to background.

Following the background measurement, the source was placed on top of the HDPE shield to minimize the distance to the detector and counted for 15 hours. The source was placed within the HDPE shield and counted for 15 hours. As expected, the number of counts in the minimalist configuration was much larger than the number of counts with the source farther from the detector, as seen in Figure 3.3.

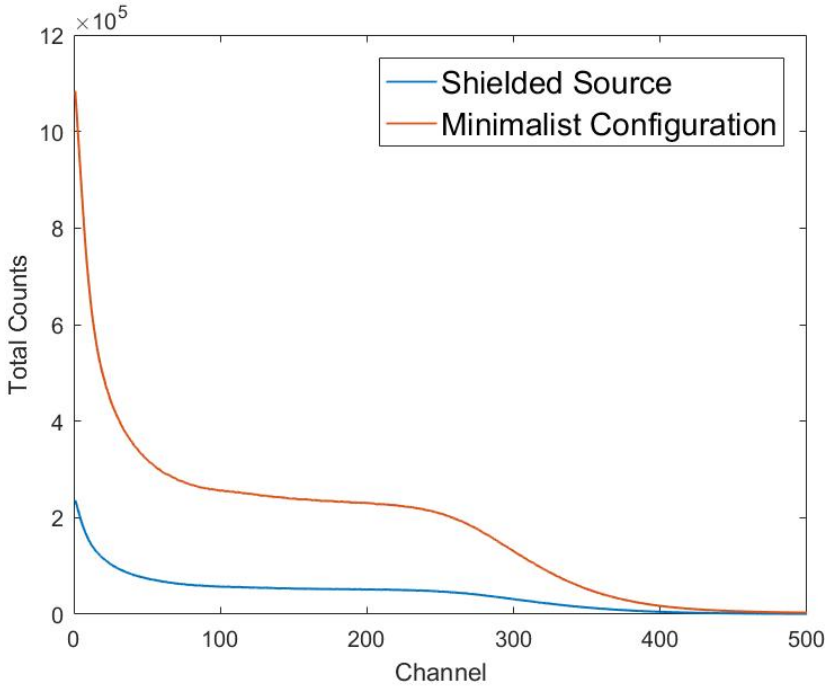

Figure 3.3: Response of proton recoil detector to two different source distances

It was not expected that the distance of the source to the detector would affect the overall shape of the spectrum, but the normalized shape is shown to be the same as seen in Figure 3.4. The major difference between the two visually is that the minimalist configuration spectrum appears to be shifted left. This is evident up to channel 100, and between channel 250 and 400. The maximum difference of 24.5% between the two spectra was located at channel 394 where the shielded source had a relative value of 0.058 and the minimalist spectrum had a relative value of 0.0494.

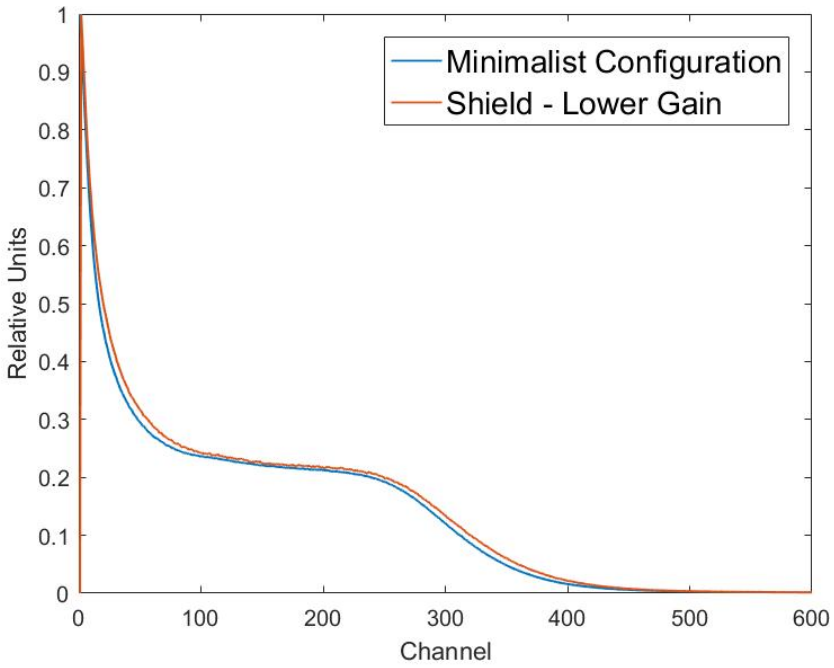

Figure 3.4: Normalized response of proton recoil detector to two different source distances

The background spectrum was subtracted from the source in the shield spectrum, but since there were so few counts in the background spectrum compared to the source spectrum, there were not any major changes within the background corrected spectrum. The largest difference between source in shield spectrum and background corrected spectrum is 11.04% at channel 43. Overall, the difference between the two spectra was most visually evident up to channel 300. Over the entire spectrum, the maximum different between the two spectra was 14.1% at channel 508. The spectra can be seen in Figure 3.5.

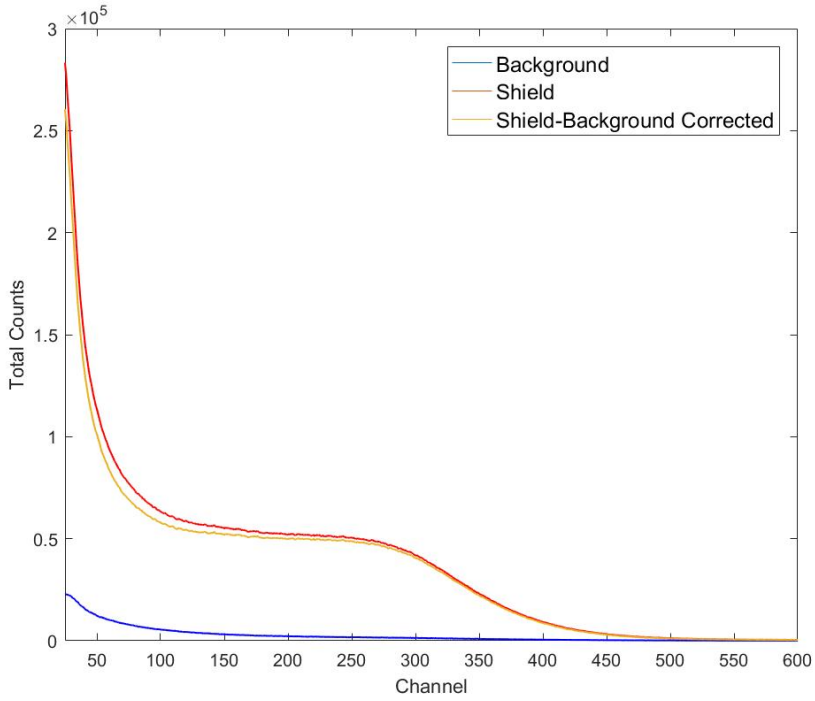

Figure 3.5: Background subtracted spectrum.

Following these measurements, the coarse gain was increased from 100 to 200 and counted for 15 hours. By increasing the coarse gain, the spectrum is observed over a larger number of channels, allowing features to be spread over a larger area. Changing the coarse gain scales the spectrum linearly, so the spectrum with the coarse gain set at 100 is able to be matched with a spectrum with the coarse gain set at 200. The largest difference between the neutron spectrum with the gain at 200 and the scaled neutron spectrum with the gain at 100 was calculated to be 6.2%, and is seen at channel 1024. The three spectra are shown in Figure 3.6.

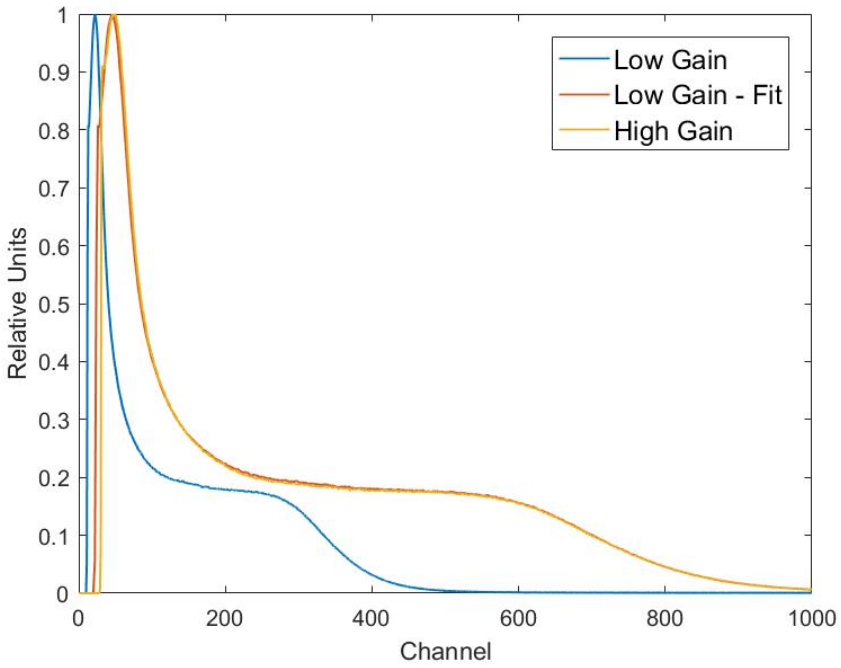

Figure 3.6: Proton recoil response with the coarse gain adjusted from 100 to 200.

3.2 MCNP

Initially, the MCNPX input deck was run without the use of the PHL tally modifier and while the F8 tally for neutrons produced results, the F8 tally for the protons failed to produce any results outside of a value in a single bin. The PHL tally modifer works by linking the F8 tally with the F6 tally and can combine the results from multiple cells. [16] However, when the PHL option was used in the gas and wall cells simultaneously, the result was not equal to the sum of the result with the PHL tally modifier in the gas and the PHL tally modifier in the wall. The changes due to the PHL tally modifier are shown in Figure 3.7.

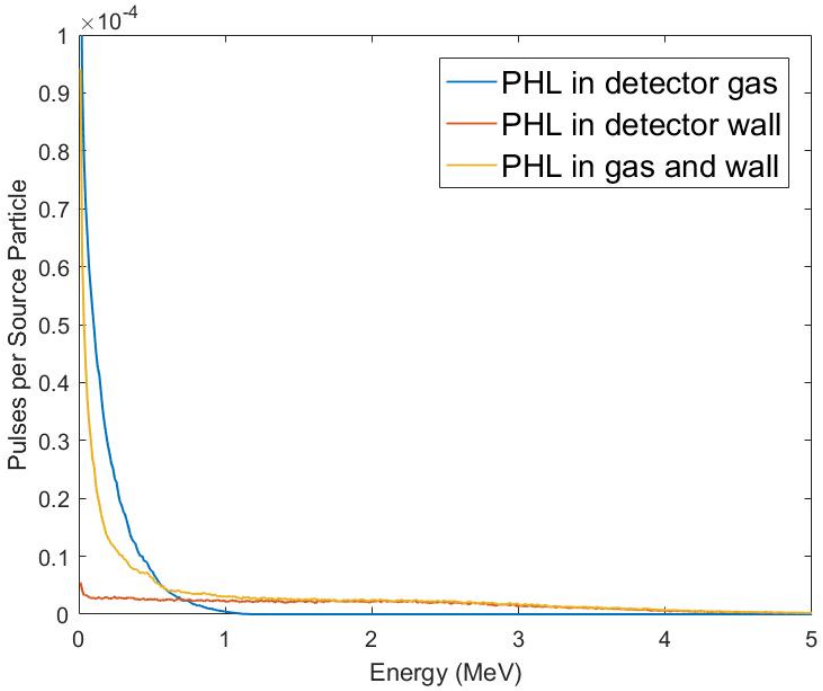

Figure 3.7: Detector response to neutron source with changes in the PHL tally modifier.

3.2.1 Response Functions

The only accessible neutron source was the ^{241}AmBe used throughout the experiment, but to determine the response functions for the proton recoil detector, monoenergetic neutrons sources were needed. As it was not possible to experimentally determine these response functions, MCNPX was used to simulate them. 120 different response functions were created ranging from 0.15 MeV to 11 MeV.

The response functions were rectangular in shape, however, at 3.03 MeV, a peak appeared at the end of the spectrum. As the initial energy of the neutron increased, the size of the peak increased, and the starting point of the peak shifted left. Protons with energies higher than 1.24 MeV have a range in the hydrogen gas larger than the

diameter of the detector. Once the proton reaches the wall, the remaining energy is deposited within the wall which shows up as the peak seen in the response functions.

At approximately 0.055 MeV, the stopping power of a proton reaches a maximum and the stopping power decreases as the energy of the proton increases. [15] Lower energy protons will deposit more of their energy within the detector volume, but the higher energy protons have a lower stopping power and will deposit less energy within the detector volume, and will be depositing more energy within the detector wall.

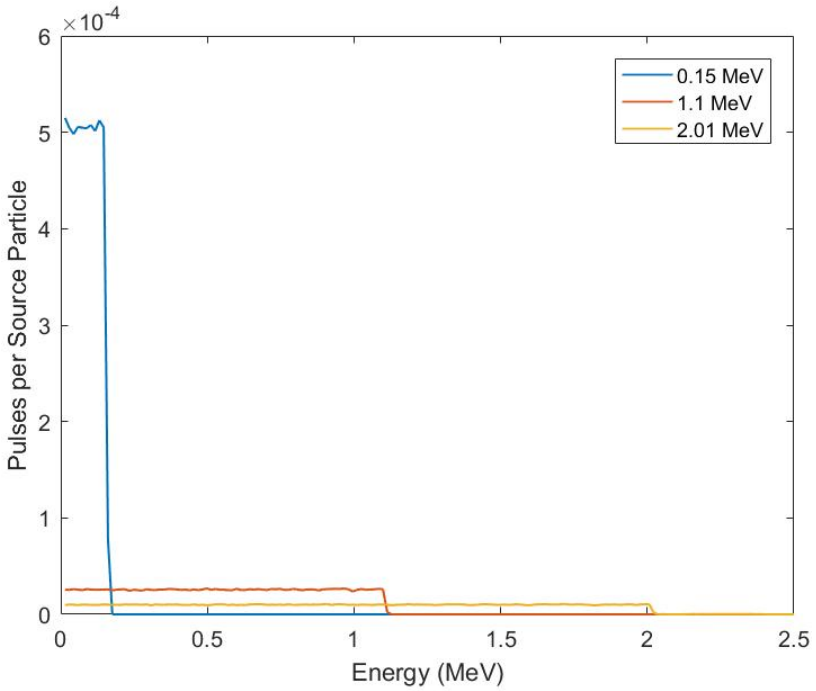

Figure 3.8: Response function for specified incident neutrons up to 2.01 MeV.

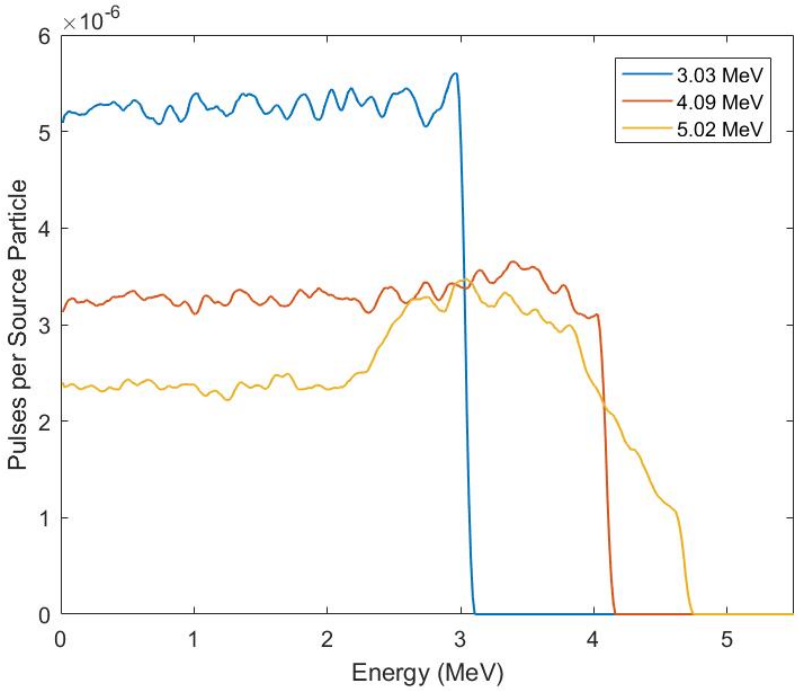

Figure 3.9: Response function for specified incident neutrons between 3.03 MeV and 5.02 MeV.

3.2.2 ^{241}AmBe Source to MCNP

Following the addition of the PHL tally modifier, the F8 tally for protons produced a spectrum that was similar to the experimental spectrum, but the MCNPX result had an additional large peak at 1.7 MeV as seen in Figure 3.10.

It was found that the ^{241}AmBe spectrum that was used in the sdef card had an error that resulted in a majority of neutrons being emitted at energies above 8 MeV. After discovering this error, an ^{241}AmBe spectrum obtained from Dr. Sunil Chirayath from the Monte Carlo Methods course was used to test whether the experimental spectrum matches that of MCNPX with an ^{241}AmBe source. The ^{241}AmBe neutron spectrum is shown in Figure 3.11.

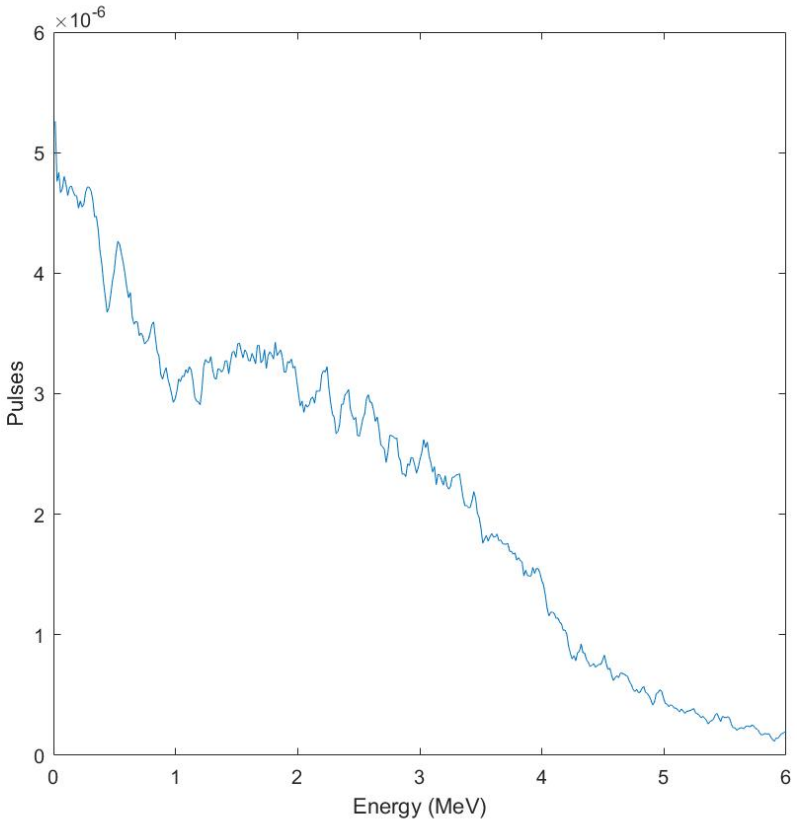

Figure 3.10: MCNPX F8 proton tally response to the incorrect ^{241}AmBe source.

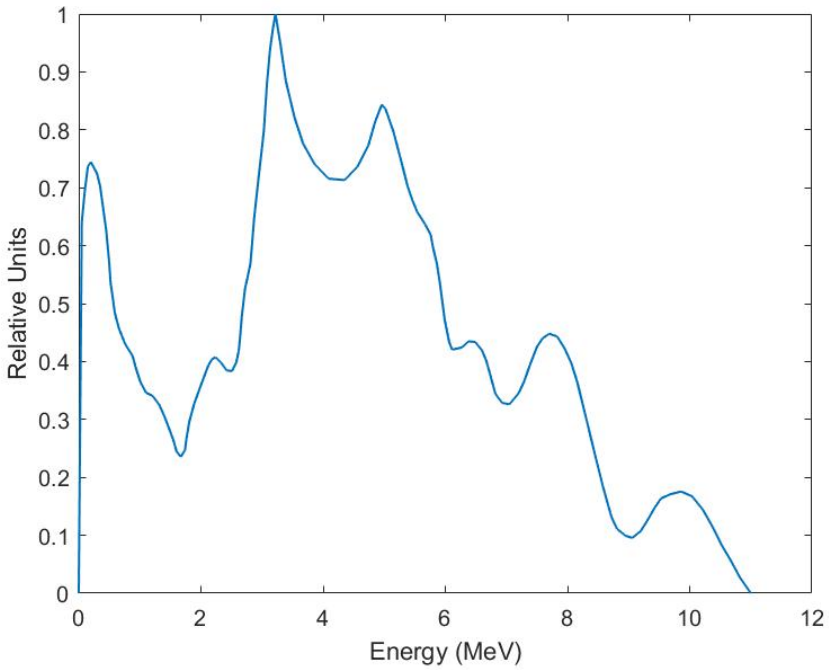

Figure 3.11: NUEN630 neutron spectrum.

The calculated and experimental spectra were normalized, and then plotted together. The experimental results were not energy calibrated and only presented as a function of channel while the calculated results were presented as a function of energy. Each bin in the calculated results was assigned a channel, but in doing so, features that were present in both spectra were located at different channels. The calculated spectrum was held steady while the experimental spectrum was scaled to match the calculated spectrum by adjusting the width of each channel. The difference was calculated between the two spectra until it reached a minimum and that determined the best fit.

After running the input deck with the new spectrum, the peak at 1.7 MeV disappeared and the resulting spectrum was similar to what was collected experimentally

as seen in Figure 3.12.

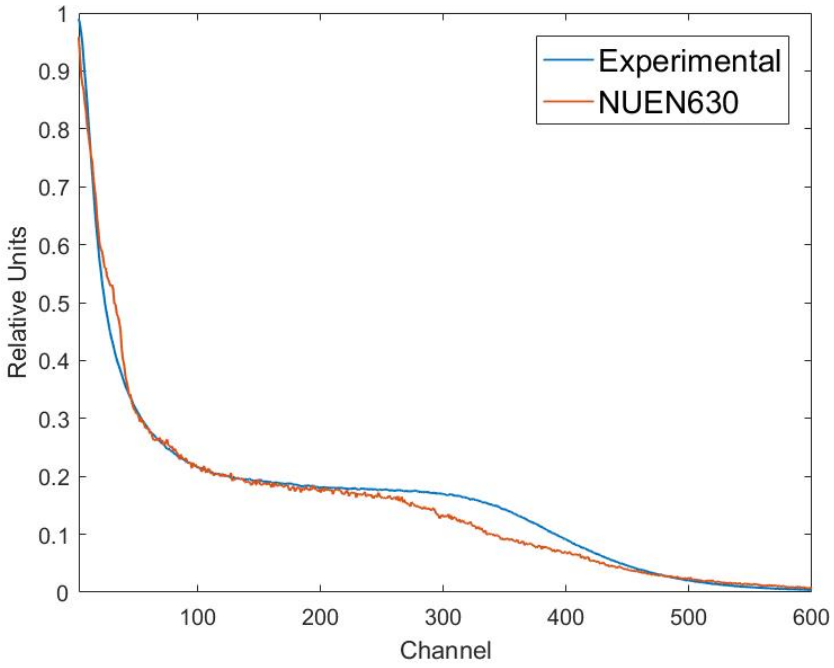

Figure 3.12: MCNPX F8 tally response to NUEN630 neutron spectrum.

The MCNPX spectrum matches the experimental spectrum well, except at two locations. Between channels 25 and 39, the calculated spectrum deviates from the measured spectrum by showing a sudden increase in the relative number of counts. Between channels 39 up to approximately channel 265, the two spectra fit well and had a difference no larger than 6%. After channel 265, the flat region of the calculated spectrum starts to decline before the measured spectrum does at approximately channel 300. Over the entire spectrum, the largest difference between the measured and calculated response was 34.9% at channel 346.

A new ^{241}AmBe spectrum was generated that corrected the mistake of the initial

neutron spectrum and was inserted into the deck. The two ^{241}AmBe spectra can be seen in Figure 3.13.

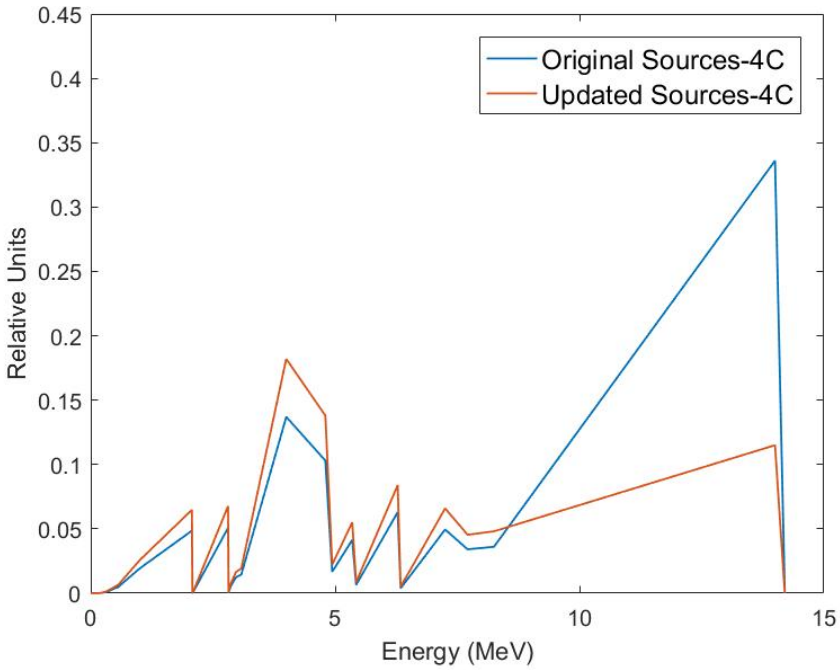

Figure 3.13: Sources-4C neutron spectra - old and new.

The major differences between the Sources-4C spectrum and the experimental spectrum occur between channel 6 and channel 125. At lower energies, the Sources-4C spectrum is concave up to channel 130, whereas the experimental spectrum is convex up until channel 231. This difference in concavity prevented the experimental and MCNPX generated spectra from matching at the lower channels up to channel 92. Between channels 155-300 and 396-522, the MCNPX and experimental results were more well-matched, with the largest difference between the two spectra being 24.2% at channel 60.

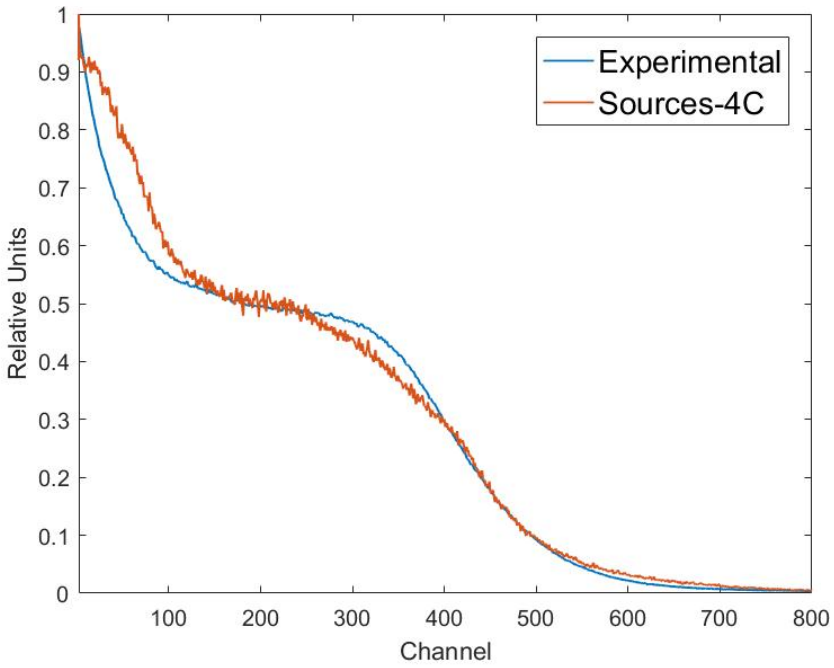

Figure 3.14: Sources-4C result compared with experimental results.

A third ^{241}AmBe spectrum, seen in Figure 3.15, was obtained from LANL that was created using ISO-8529 as a reference.

The resulting spectrum differed the most from the experimental spectrum as seen in Figure 3.16. Between channels 100 and 300, the experimental spectrum contains a shelf while the calculated spectrum is constantly decreasing with a larger slope. The two response spectra were able to match well at the lower end up to channel 23 and at the higher end after channel 500. The largest differences between the spectra, 28.8% and 21%, occurred at channel 77 and channel 323.

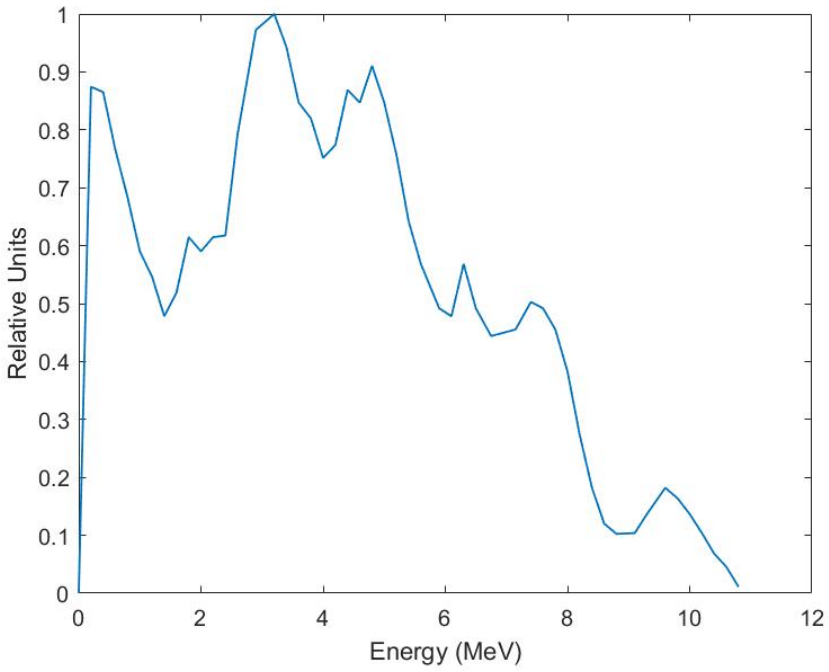

Figure 3.15: LANL neutron spectrum created from ISO-8529 neutron spectrum.

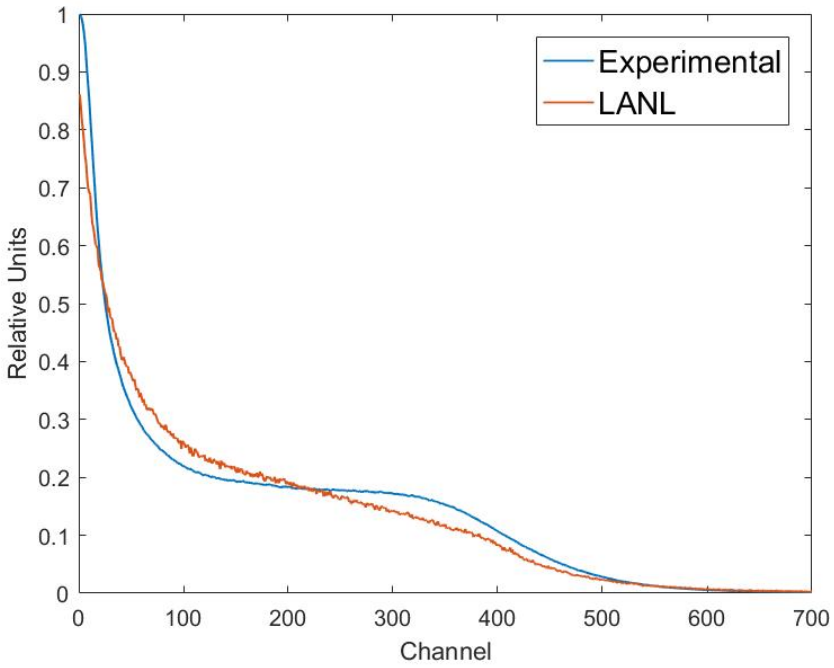

Figure 3.16: LANL result compared with experimental results.

The three neutron spectra that were used can be seen in Figure 3.17. The NUEN630 and LANL spectra have very similar shapes, but the main difference between the two is the probability of a neutron being emitted at certain energies. Both have a maximum at 3.2 MeV and show that no neutron is emitted at an energy higher than 11 MeV, but especially in the energy region up to 3.2 MeV, the LANL spectrum has more neutrons being emitted at lower energies than the NUEN630 spectrum. The Sources-4C neutron spectrum shared a few similarities with the other two ^{241}AmBe neutron spectra such as the location of local maximum, but the maximum of the Sources-4C spectrum was located at 4 MeV which is where the other spectra have a local minimum. The major difference between the Sources-4C neutron spectrum and the previous two neutron spectra is that the Sources-4C has neutrons

being emitted at energies up to 14 MeV, whereas the others emit nothing higher than 11 MeV neutrons. In addition, over 57% of neutrons were emitted at energies higher than 7.71 MeV in the Sources-4C spectrum, where at most, 14% of neutrons were emitted at energies higher than 7.71 MeV in the NUEN630 and LANL spectra.

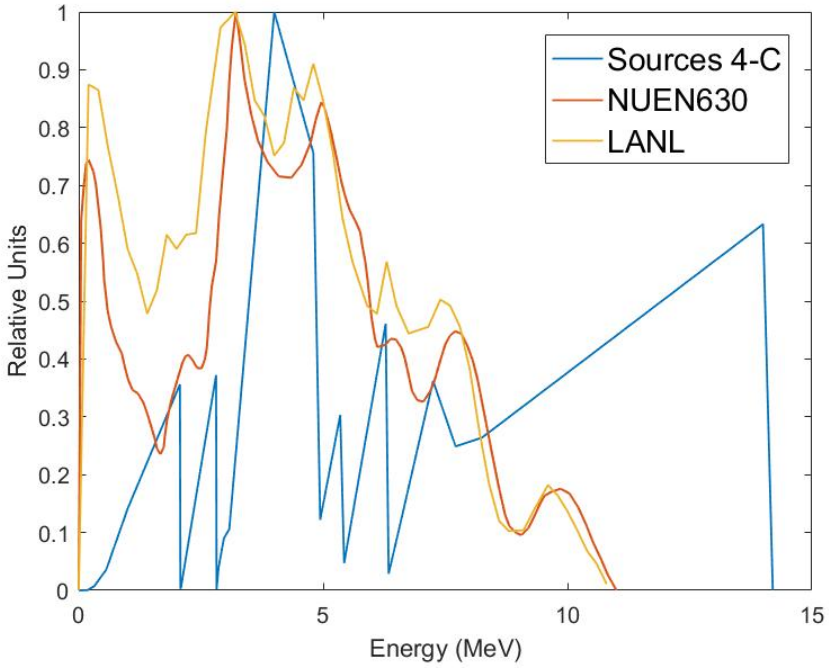

Figure 3.17: Various ^{241}AmBe neutron spectra.

3.2.3 Mixed ^{241}AmBe Sources

To observe which energy ranges affected the detector response to the ^{241}AmBe source, two new neutron spectra were created by merging features from the LANL and NUEN630 neutron spectra, and the Sources-4C and LANL spectra.

The main difference between the two spectra was in the energy region up to 3 MeV. The region below 3 MeV from the LANL spectrum, and the region from 3

MeV to 11 MeV from the NUEN630 spectrum were merged into a new spectrum as seen in Figure 3.18.

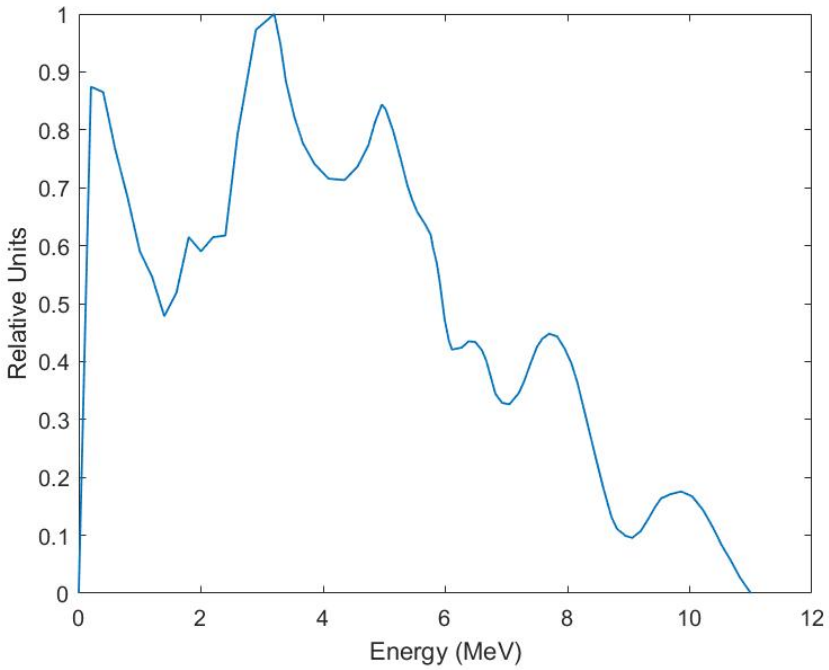

Figure 3.18: Neutron spectrum created from the LANL and NUEN630 spectrum.

The mixed source response was most similar to the LANL response up to 1 MeV, then above 1 MeV, it followed the shape of the NUEN630 response spectrum, but at a higher relative height. The three spectra can be seen in Figure 3.19.

The F8 proton tally response to the LANL-NUEN630 source was a better fit to the experimental response than either the NUEN630 or LANL spectra. Up to channel 400, the largest difference between the experimental and mixed source spectra was 18.2% at channel 275.

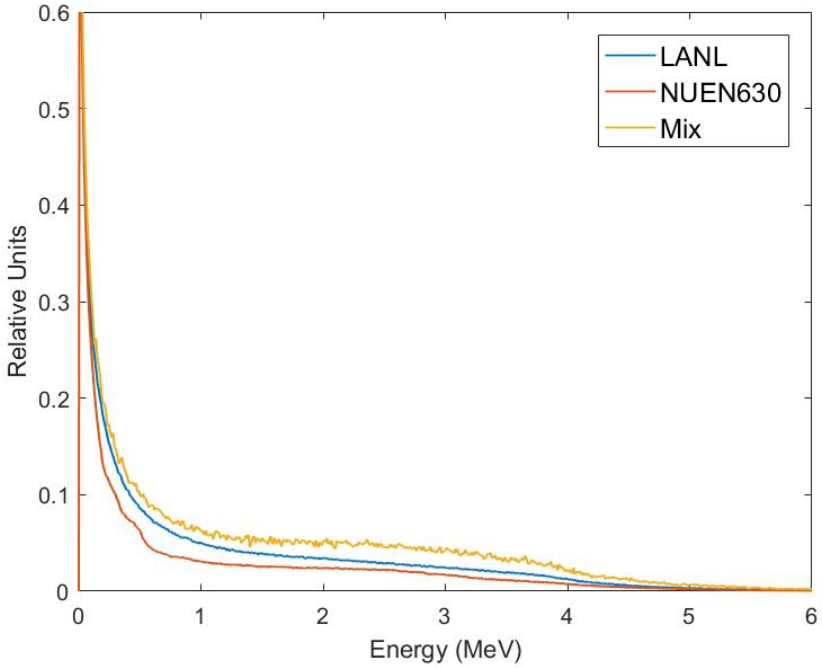

Figure 3.19: Comparision between mixed source, LANL, and NUEN630 detector response.

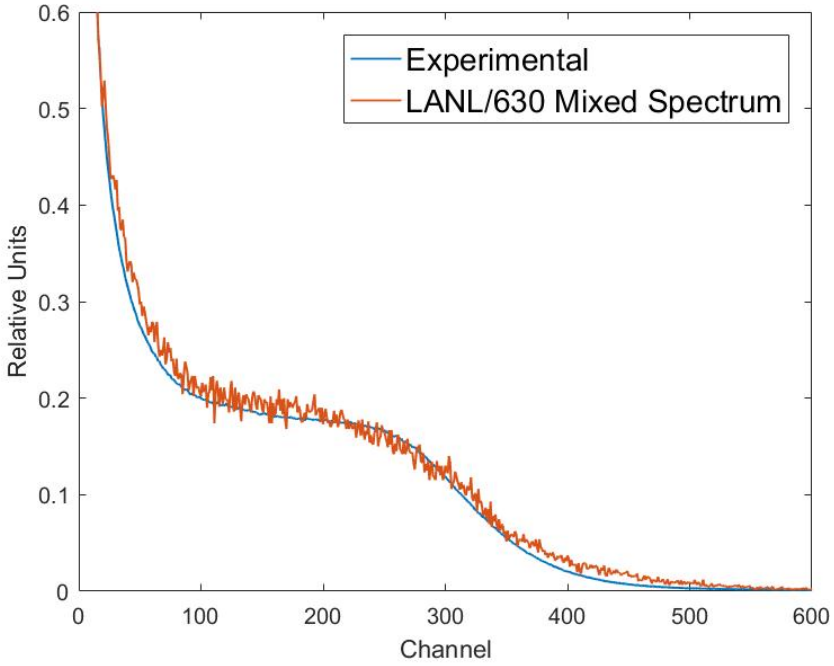

Figure 3.20: Mixed LANL-NUEN630 spectrum response fit to experimental results.

To observe the effect the region above 7.71 MeV had on the detector response, the energy region above 7.71 MeV in the Sources-4C spectrum was replaced with the LANL neutron spectrum between 8.2 MeV and 11 MeV. The mixed neutron spectrum can be seen in Figure 3.21.

The calculated response contains a local maximum at 1.71 MeV, a feature not seen in either the LANL or Sources-4C response. As with the mixed LANL and NUEN630 response spectrum, the Sources-4C and LANL spectrum response had a larger relative height than the original Sources-4C response spectrum. Changing the neutron spectrum did not result in a change in a single, isolated region, but affected the entire response.

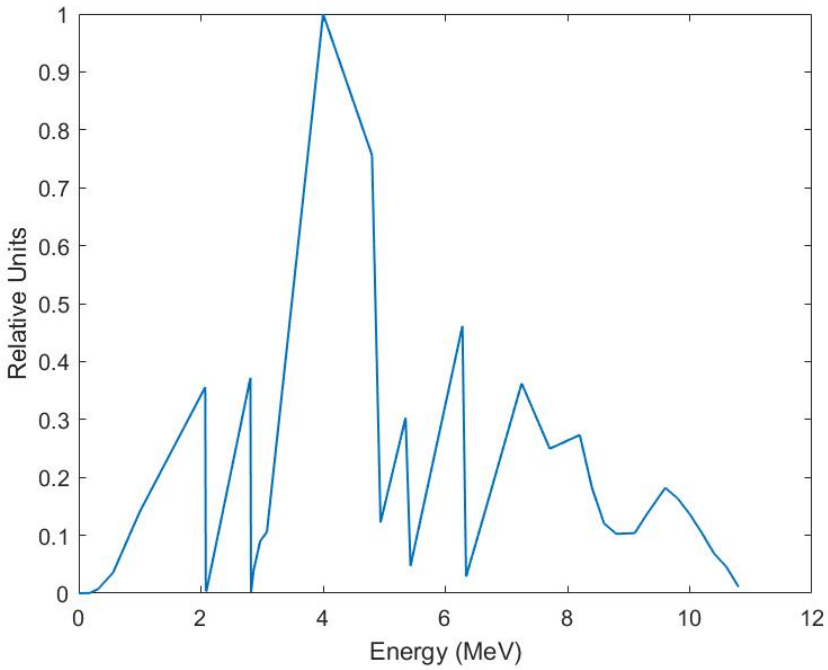

Figure 3.21: Neutron spectrum created from the LANL and Sources-4C spectrum.

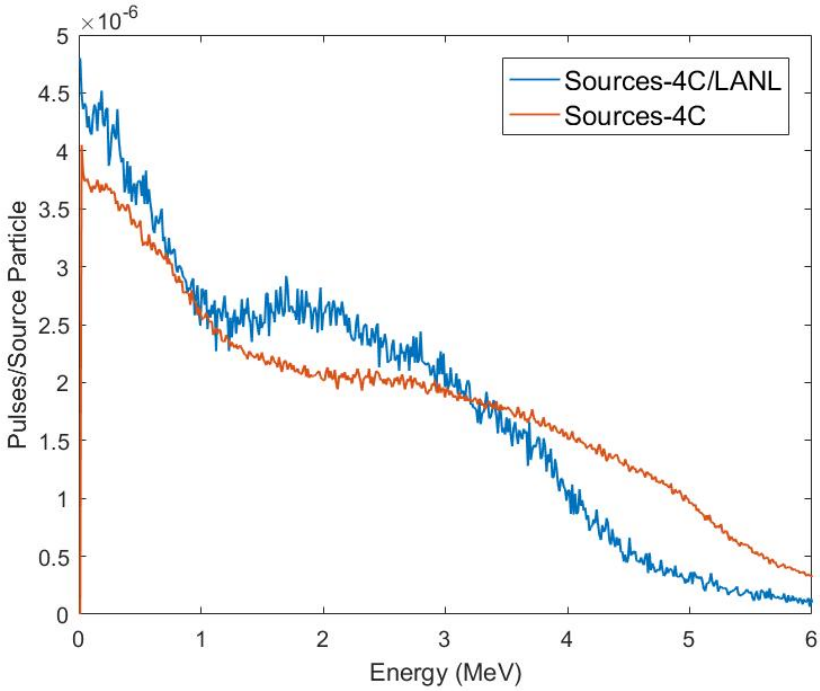

Figure 3.22: Comparison between second mixed neutron source and Sources-4C detector response.

3.2.4 Test

A simple problem of three discrete neutron energies, 0.8 MeV, 1.2 MeV, and 3.0 MeV was run in MCNPX to use as a test problem for MAXED. All three energies were emitted at a 1:1:1 ratio.

3.3 MAXED

Once the output files were generated from MCNPX, the output had to be formatted in a certain way for MAXED. Errors are magnified throughout the unfolding process, so the MCNPX calculated response functions were smoothed. [17] To facilitate this, MATLAB© was used to smooth the response functions.

3.3.1 Test

After running the result of the test file of the three discrete energies, 0.8, 1.2, and 3.0 MeV, the results were unfolded using MAXED. The result of the unfolding is shown in Figure 3.23.

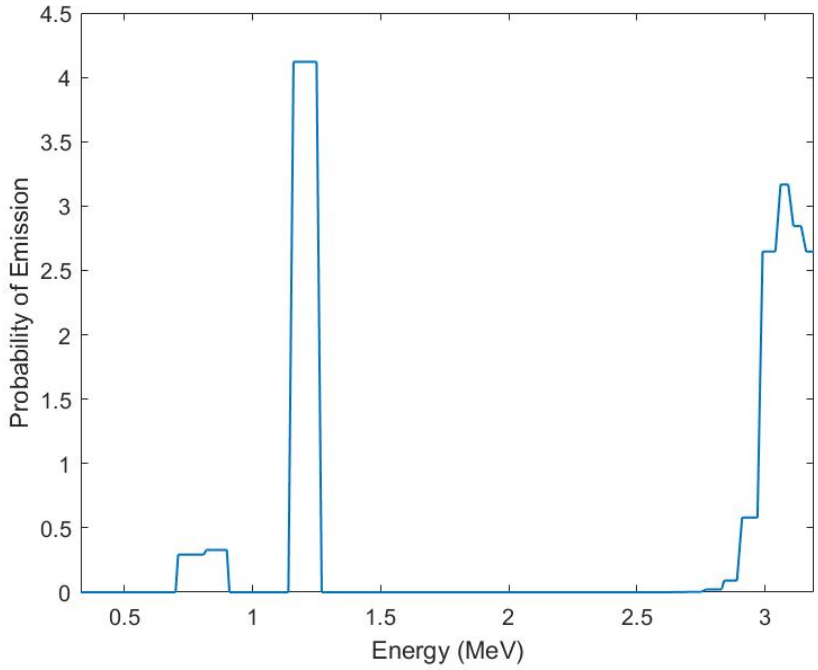

Figure 3.23: MAXED test unfolded response.

In MCNPX, each of the energies were made to be emitted 100% of the time, however that is not what is shown in MAXED. The unfolded spectrum was able to show the three emitted energies, however, rather than a pulse at the one energy, the pulse extends over a fraction of a few MeV. The first peak ranged from 0.71 MeV to 0.9 MeV with the center located at 0.8 MeV. The second peak ranged from 1.15 MeV

to 1.26 MeV with the center at 1.21 MeV, and the final peak ranged from 2.7 MeV to 3.19 MeV with the average at 2.95 MeV, but the maximum was located at 3.07 MeV. The height of each peak ranged from 0.3278 to 4.1207, a relative difference of 92% from the maximum. In addition, a .txt file was created that showed the experimental or MCNPX response compared to the response calculated by MAXED with the response functions. The results are shown in Figure 3.24.

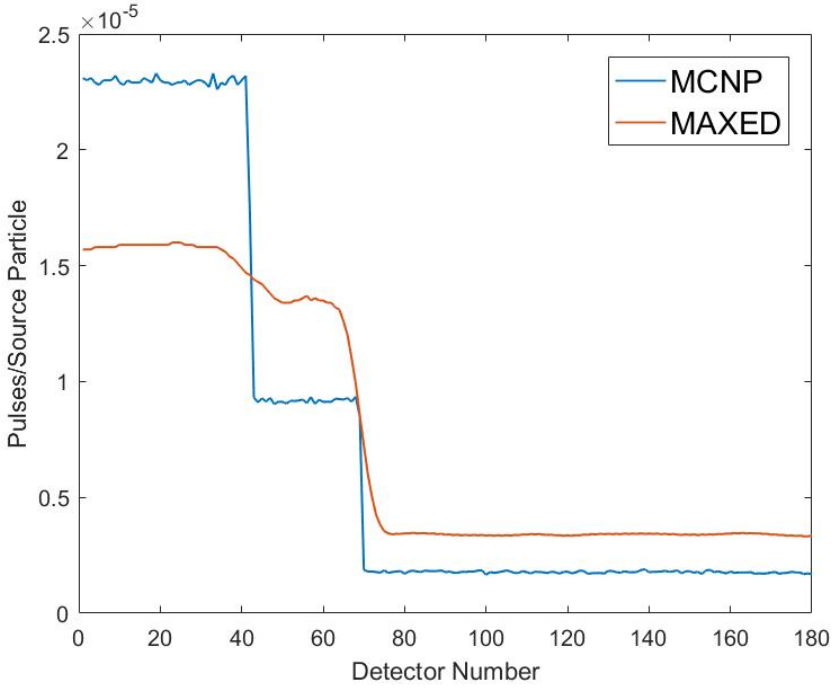

Figure 3.24: MCNPX calculated response and MAXED calculated response to three discrete energies.

The MAXED response can be seen to follow the general trend of the MCNPX calculated response, however there are large differences in the relative height of the response. The largest difference between the MCNPX and MAXED response was

found to be 288.4% at detector number 70, while at detector number 69, the relative difference between the two responses is 0.39%. The MAXED response was not able to have changes as drastic as the MCNPX response from one detector number to the next.

3.3.2 $^{241}AmBe$

Following the unfolding of the test file, MAXED was run with the experimentally collected response. The unfolded response is shown in Figure 3.25.

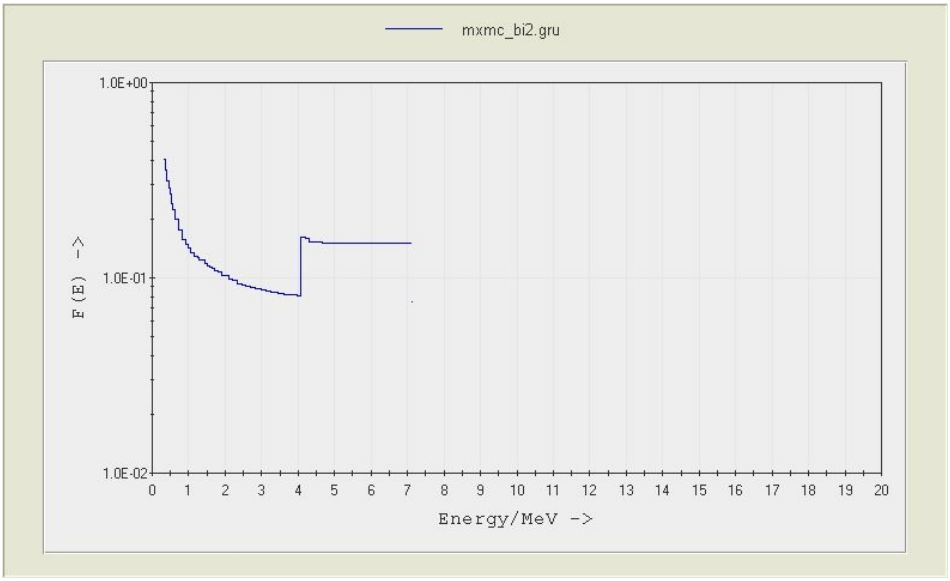

Figure 3.25: Unfolded experimental detector response.

The response was not able to be unfolded up to 11 MeV without failing to create any sort of unfolded response. The response shown in Figure 3.26 was the best estimate able to be collected from MAXED for the experimental spectrum. Unfortunately, the spectrum fails to show any resemblance to the previously shown ^{241}AmBe spectra.

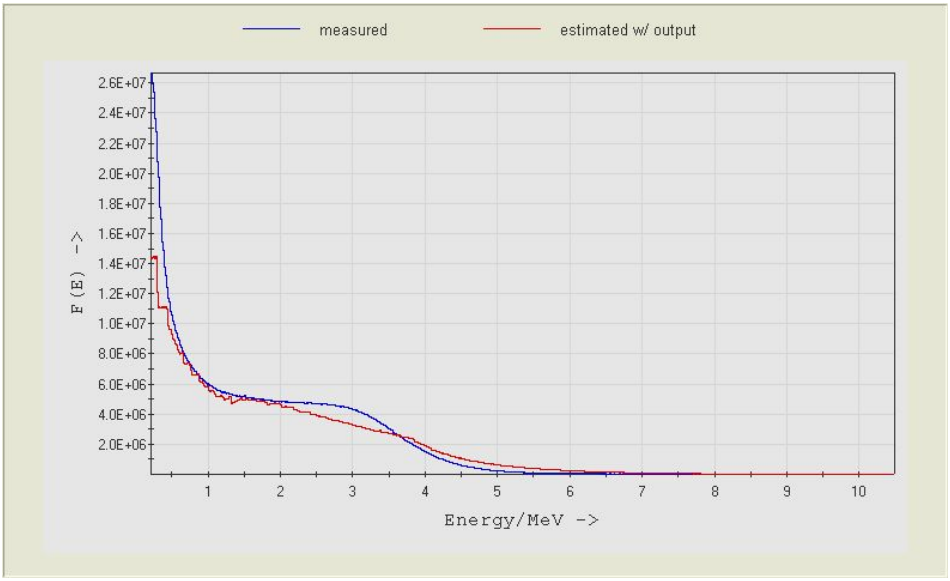

Figure 3.26: Experimental detector response and MAXED calculated response to ^{241}AmBe source.

The response file created by MAXED using the MCNPX generated response shows similarities to the experimental response, but much like the MCNPX calculated responses, the flat region of the spectrum ends too early at 2 MeV while the experimental spectrum ends at approximately 3 MeV. The results presented by MAXED are not able to determine the spectrum observed by the proton recoil detector.

4. CONCLUSION AND FUTURE WORK

4.1 Conclusion

While attempting to unfold the neutron spectrum from the proton recoil detector, there were difficulties encountered while using MAXED. MAXED has been shown to successfully unfold an ^{241}AmBe spectrum, however, when attempted with the experimental results and MCNP generated response functions, the unfolding was not successful. As mentioned before, errors are amplified through the unfolding process, so errors in the experimental and response functions could have led to the result shown. It is possible that the number of MCNP calculated response functions could have been insufficient and a larger number was needed to successfully use MAXED.

The test file with three discrete energies was able to be unfolded, but there was a large discrepancy in the relative pulse height of the emitted energies. Since the response functions used were constant between the test and experimental input files, some of the error can be attributed to the variation in the calculated response function which can possibly be resolved by running a larger number of particles.

Despite this, the experimental spectrum was able to be reproduced to a certain degree using MCNP. Three different ^{241}AmBe spectra that were collected and contained significant differences between them were able to match the experimental spectrum to a certain degree. However, when the LANL and NUEN630 spectra were combined to form a new neutron spectrum, the result was the best fit to the experimental data. The simulated detector was sensitive to changes in the neutron spectrum as the calculated responses show. While the LANL and NUEN630 spectrum follows the shape of the ^{241}AmBe ISO standard and best fits the experimental data, it does not necessarily mean that is the neutron spectrum that the proton recoil

detector is measuring. Further attempts can be made to minimize the error in the response functions and to create more response functions so the measured neutron spectrum can be unfolded and compared with known ^{241}AmBe source spectra.

4.2 Future Work

As mentioned earlier, the experiments were performed under changing conditions. Future results should all be performed under the same conditions, most likely over the weekend when the reactor at the Nuclear Science Center is guaranteed to be off. More work can be done to reduce the statistical error associated with the MCNP calculations by executing the code with a larger number of histories or through variance reduction techniques. A larger number of response functions could be what is needed to successfully unfold the neutron spectrum. In simulations, the different neutron spectra result in different count rates, so MCNP can be run with the different neutron spectra and the count rates between the simulation and experiment can be compared. In addition, work is being done to improve the MCNP input deck and resolve any errors that were not previously noticed.

REFERENCES

1. Crane, T.W., and M.P. Baker. "Passive Nondestructive Assay Manual." Los Alamos National Laboratory, New Mexico, pp. 379, 384
2. Knoll, Glenn F. *Radiation Detection and Measurement 4th ed.*. New York, New York: Wiley, 2010, pp. 54, 159-160, 534, 569-578, 725-726
3. Lamarsh, John R. *Introduction to Nuclear Reactor Theory.* Reading, Massachusetts: Addison-Wesley Pub., 1966, pp. 53-54
4. Kreyszig, Erwin, *Advanced Engineering Mathematics 10th ed.* New York, New York: J. Wiley & Sons, 2011, pp. 232
5. Tsoulfanidis, Nicholas. *Measurement and Detection of Radiation 2nd ed.*. Washington, D.C.: Taylor & Francis, 1995, pp. 304-305
6. Reginatto, Marcel, "The 'Multi-Channel' Unfolding Programs in the UMG Package: MXD_MC33, GRV_MC33 and IQU_MC33." Physikalisch-Technische Bundesanstalt (PTB), Braunschweig, Germany.
7. Pehlivanovic, B. Avdic, S., Marinkovic, P., Pozzi, S.A., Flaska, M.,"Comparison of Unfolding Approaches for Monoenergetic and Continuous Fast-Neutron Energy Spectra." Radiation Measurements, 49(2013):109-114.
8. D.B. Pelowitz, Ed., "MCNPX Users Manual Version 2.7.0." LA-CP-11-00438, Los Alamos National Laboratory, New Mexico.
9. Pozzi, Sara, Padovani, Enrico, Marseguerra, Marzio, "MCNP-PoliMi: A Monte-Carlo Code for Correlation Measurements." Nuclear Instruments and Methods in Physics. 513(2003):550-558.
10. Murata, Isao, Iehito Tsuda, Ryotaro Nakamura, Shoko Nakayama, Masao Matsumoto, and Hiroyuki Miyamaru. "Neutron and Gamma-ray Source-term

Characterization of AmBe Sources in Osaka University." Progress in Nuclear Science and Technology. 4(2014):345-48.

11. Pujala, Usha, Selvakumaran, T.S., Mohapatra, D.K., Raja, E. Alagu, Subbaiah, K.V., Baskaran, R. "Analysis of Neutron Streaming Through the Trenches at LINAC Based Neutron Generator Facility, IGCAR." Indian Association for Radiation Protection, 34(2011):262-266.
12. Monsanto Research Corporation, ^{241}AmBe Source Specification Sheet, (1972).
13. LND, Inc. 27044 Spherical Proton Recoil Neutron Detector Specification Sheet.
14. Durkee Jr., Joe W., James, Michael R., McKinney, Gregg W., Waters, Laurie S., Goorley, John T., "The MCNP6 Delayed Particle-Feature." LA-UR-12-00283, Los Alamos National Laboratory, New Mexico.
15. Berger, M.J., J.S. Coursey, M.A. Zucker, and J. Chang. "PSTAR: Stopping Power and Range Tables for Protons." Stopping-Power and Range Tables for Electrons, Protons, and Helium Ions. NIST, 7 Oct. 2009.
16. Fensin, Michael Lorne, McKinney, Gregg W., "How to Use the MCNP6 Background Source Capability." LA-UR-13-23344, Los Alamos National Laboratory, New Mexico.
17. Su, Y. S, "Study of Scintillation Spectrometry: Unfolding Methods." Nuclear Instruments and Methods, 54(1967):109-115.

APPENDIX

The following are the files used to execute MCNP and MAXED. The first file is shown in the MCNP input deck, the second file is the control file that was used to execute MAXED.

```
HPH Detector
c ---------------------------------- Cell Cards ---------------------------------
60   7   -7.92        -611 610     imp:n=1 imp:h=1
61   10  -2.469E-4    -610         imp:n=1 imp:h=1
62   6   -0.0012048   -615 611     imp:n=1 imp:h=1
c 62   3   -0.95        -612 611   imp:n=1 imp:h=1
c 63   8   -3.3831      -613 612   imp:n=1 imp:h=1
c 64   3  -0.95         -614 613   imp:n=1 imp:h=1
c 9999 0                 614        imp:n=0 imp:h=0
9999 0                 615          imp:n=0 imp:h=0

c --------------------------------- Surface Cards ------------------------------
c BF3 Detector Sphere
610 so  +2.535
611 so  +2.54
c 612 so  +12.54
c 613 so  +15.04
c 614 so  +25.04
615 so   +6.00

c ----------------------------------- Data Cards -------------------------------
c ************************* Bounds *************************
mode  N H P #
c imp:# 1 1 1 0
c RAND STRIDE=102917
print 110
phys:n j 100 3J -1 1
phys:h j 20 4j 0.9
cut:N  2J 0 0
cut:h j 0
nps 2E9sss
c ******************* Material Definitions ******************
c Stainless Steel
m7      024052.80c   1.7428E-2
        025055.80c   1.7363E-3
        026056.80c   5.9358E-2
        028058.80c   7.7199E-3
c High Pressure Hydrogen
m10     001001.80c   1
c HDPE
m3      001001.80c   8.1570E-2
        006000.80c   4.0787E-2
mt3     poly.10t
c Air
m6      006000.70c   7.4906E-9
        007014.70c   3.9123E-5
        008016.70c   1.0511E-5
        018040.70c   2.3297E-7
c AmBe Source
m8      095241.70c   1.1649E-3
        008016.70c   2.3298E-3
        004009.70c   1.9077E-1
c ********************** Source Definition ******************
SDEF  pos=0 0 -4.54  AXS= 0 0 1 EXT=0 rad=d1 erg=1.01 PAR=1
      VEC=0 0 1   DIR=1
c SI1 12.54 15.04
SI1 0 2.6
SP1 -21 1
c LANL AmBe spectrum - 4/19/2016
si3  H    0  0.2   0.4   0.6   0.8   1.0   1.2    1.4   1.6
             1.8   2.0   2.2   2.4   2.6   2.9    3.2   3.4
             3.6   3.8   4.0   4.2   4.4   4.6    4.8   5.0
             5.2   5.4   5.6   5.9   6.1   6.3    6.5   6.75
             7.15  7.4   7.6   7.8   8.0   8.2    8.4   8.6
             8.8   9.1   9.3   9.6   9.8   10.0   10.2  10.4
             10.6   10.8
sp3  D    0   0.16     0.1583   0.14     0.125   0.108   0.10
             0.0875   0.095    0.1125   0.108   0.1125
             0.113    0.145    0.178    0.183   0.1725  0.155
             0.15     0.1375   0.1416   0.159   0.155   0.1666
             0.155    0.1385   0.1175   0.104   0.09    0.0875
             0.104    0.09     0.08125  0.08333 0.092   0.09
             0.08333  0.07     0.05     0.03333 0.022   0.01875
             0.019    0.025    0.0333   0.03    0.025   0.019
             0.0125   0.008333 0.002
```

```
c SI3 H  0.00000E+00 1.82202E-09 4.97106E-09 6.18000E-09 7.28878E-09
c        8.61545E-09 9.06000E-09 1.14000E-08 1.35465E-08 1.36000E-08
c        1.53687E-08 1.55000E-08 1.74000E-08 1.92000E-08 2.08353E-08
c        2.10000E-08 2.28000E-08 2.45000E-08 2.63000E-08 2.80000E-08
c        2.97000E-08 2.99463E-08 3.15000E-08 3.33000E-08 3.51000E-08
c        3.70000E-08 3.89000E-08 4.08000E-08 4.28000E-08 4.29973E-08
c        4.49000E-08 4.70000E-08 4.93000E-08 5.16000E-08 5.40000E-08
c        5.66000E-08 5.93000E-08 6.22000E-08 6.53000E-08 6.87000E-08
c        7.23000E-08 7.64000E-08 8.09000E-08 8.60000E-08 9.20000E-08
c        9.92000E-08 1.08000E-07 1.21000E-07 1.42000E-07 1.84000E-07
c        2.38000E-07 3.09000E-07 4.00000E-07 5.62341E-07 1.00000E-06
c        1.77828E-06 3.16228E-06 5.62341E-06 1.00000E-05 1.77828E-05
c        3.16228E-05 5.62341E-05 1.00000E-04 1.77828E-04 3.16228E-04
c        5.62341E-04 1.00000E-03 1.77828E-03 3.16228E-03 5.62341E-03
c        1.00000E-02 1.77828E-02 3.16228E-02 5.62341E-02 1.00000E-01
c        1.77828E-01 3.16228E-01 5.62341E-01 1.00000E+00 2.07016E+00
c        2.07831E+00 2.08769E+00 2.81313E+00 2.81512E+00 2.86312E+00
c        2.97494E+00 3.08125E+00 4.00230E+00 4.80107E+00 4.94256E+00
c        5.35484E+00 5.43000E+00 6.27650E+00 6.33875E+00 6.57250E+00
c        7.24687E+00 7.71093E+00 8.25392E+00 1.40000E+01 1.42000E+01
c SP3 D  0.00000E+00 1.52838E-12 2.65612E-12 1.01970E-12 9.35222E-13
c        1.11901E-12 3.74964E-13 1.97372E-12 1.81051E-12 4.51256E-14
c        1.49184E-12 1.10748E-13 1.60259E-12 1.51825E-12 1.37933E-12
c        1.38919E-13 1.51825E-12 1.43390E-12 1.51825E-12 1.43390E-12
c        1.43390E-12 2.07747E-13 1.31050E-12 1.51825E-12 1.51825E-12
c        1.60259E-12 1.60259E-12 1.60259E-12 1.68694E-12 1.66417E-13
c        1.60487E-12 1.77129E-12 1.93998E-12 1.93998E-12 2.02433E-12
c        2.19302E-12 2.27737E-12 2.44606E-12 2.61476E-12 2.86780E-12
c        3.03649E-12 3.45823E-12 3.79561E-12 4.30169E-12 5.06082E-12
c        6.07298E-12 7.42253E-12 1.09651E-11 1.77129E-11 3.54257E-11
c        4.55474E-11 5.98863E-11 7.67557E-11 1.36930E-10 3.69152E-10
c        6.56456E-10 1.16736E-09 2.07589E-09 3.69152E-09 6.56456E-09
c        1.16736E-08 2.07589E-08 3.69152E-08 6.56456E-08 1.16736E-07
c        2.07589E-07 3.69152E-07 6.56456E-07 1.16736E-06 2.07589E-06
c        3.69152E-06 6.56456E-06 1.16736E-05 2.07589E-05 3.69152E-05
c        6.56456E-05 1.30253E-03 6.48573E-03 2.56416E-02 6.47634E-02
c        6.15753E-04 7.08682E-04 6.76703E-02 2.91153E-04 7.02278E-03
c        1.63602E-02 1.92567E-02 1.82000E-01 1.37627E-01 2.22283E-02
c        5.51467E-02 8.56286E-03 8.39532E-02 5.22571E-03 2.03472E-02
c        6.59330E-02 4.54000E-02 4.80575E-02 1.15250E-01 0.00000E+00
```

```
c Dr. Sunil AmBe "spectrum"
c si3 H  0.000  0.050  0.100  0.150  0.200  0.300
c        0.350  0.450  0.500  0.520  0.550  0.590
c        0.660  0.760  0.880  0.940  1.010  1.100
c        1.210  1.320  1.400  1.470  1.550  1.600
c        1.670  1.740  1.760  1.810  1.890  2.010
c        2.120  2.180  2.240  2.330  2.420  2.510
c        2.580  2.620  2.640  2.670  2.720  2.810
c        2.830  2.870  2.940  3.030  3.080  3.130
c        3.180  3.220  3.300  3.390  3.530  3.670
c        3.860  4.090  4.350  4.560  4.740  4.850
c        4.960  5.020  5.150  5.270  5.380  5.460
c        5.540  5.670  5.760  5.800  5.860  5.910
c        5.990  6.060  6.110  6.270  6.380  6.490
c        6.600  6.670  6.740  6.820  6.930  7.050
c        7.200  7.290  7.390  7.500  7.590  7.700
c        7.830  7.950  8.060  8.160  8.310  8.450
c        8.580  8.720  8.810  8.950  9.060  9.200
c        9.320  9.430  9.530  9.680  9.860 10.040
c       10.220 10.380 10.520 10.680 10.820 11.000
c SP3 D    0.000 10.720 11.640 12.340 12.460 12.120
c         11.760 10.480  9.520  8.980  8.620  8.100
c          7.640  7.200  6.860  6.480  6.100  5.800
c          5.700  5.440  5.120  4.800  4.420  4.100
c          3.940  4.140  4.440  4.960  5.480  6.060
c          6.580  6.760  6.820  6.660  6.440  6.420
c          6.680  7.020  7.380  8.020  8.780  9.520
c          9.940 10.820 11.960 13.360 14.720 15.700
c         16.340 16.740 15.880 14.800 13.760 13.000
c         12.400 11.980 11.940 12.320 12.940 13.620
c         14.120 14.000 13.340 12.540 11.780 11.360
c         11.020 10.660 10.360  9.980  9.540  8.980
c          7.900  7.280  7.040  7.100  7.280  7.260
c          7.020  6.720  6.280  5.760  5.500  5.460
c          5.780  6.120  6.620  7.120  7.360  7.500
c          7.420  7.080  6.660  6.100  5.020  4.000
c          3.080  2.200  1.860  1.660  1.600  1.800
c          2.140  2.480  2.740  2.860  2.940  2.800
c          2.400  1.900  1.400  0.920  0.460  0.000
c ************************* Tallies ************************
c detector tallies
F6:h    61            $Energy Deposited for Proton in detector
E6 0 250i 15
F16:h    60            $Energy Deposited for Proton in detector wall
E16 0 250i 15
F8:h     61
FT8      PHL 2 6 1 16 1 0
E8  0 1023i 15
c Neutron Energy Deposition
F26:n    61            $Energy Deposited for neutron in detector
E26 0 250i 15
F36:n    60            $Energy Deposited for neutron in detector wall
E36 0 250i 15
F18:n     61
FT18      PHL 2 6 1 16 1 0
E18  0 1023i 15
c analog
F28:h    61
FT28     CAP
```

```
LANL.phs                                  file with data
..\..\$inp\response\may24a.rsp            file with response functions (RF)
mxmc_bi2                                  name of output file
..\..\$inp\def_spec\flat_fine.flu         file with default spectrum (DS)
0.2,7.0                                   lo, hi MC E bin edges (in MC E units)
0.33,7.15                                  lo, hi RF E bin edges (in MeV)
2.55                                      chi-square factor
20000                                     Maximum number of iter. in L-BFGS-B
3,1                                       3 = use RF bin structure, 1 = dF/dE
1                                         1 = use a scale factor for the DS
0                                         0 = use MAXED scale factor
```